EDIT 2015
INTERNATIONAL SCHOOL
FRASCATI - OCT.20-29

Excellence in Detectors and Instrumentation Technologies

Beam Infrared Detection with Resolution in Time

Alessandro Drago

INFN - Laboratori Nazionali di Frascati, Italy
October 20-29, 2015

Introduction

- Electron and positron beams stored in last generation circular accelerators, both used as light sources and as colliders, need power diagnostics systems to evaluate and to characterize the behaviour of the stored charges. These are gathered in bunches of the order of 10^9 – 10^13 particles showing usually shapes that in first approximation are Gaussian in the three dimensions. The bunches run through the vacuum chamber at light speed in h equilibrium points (called buckets) to maintain the synchronous phase with the strong RF (radio frequency) sinusoidal fields restoring every turn the lost beam energy. The h number is called harmonic and it is given by the ratio between the RF frequency and the ring revolution frequency.
- Many diagnostics systems allow the accelerator physicists to check the beam performance driving the working conditions towards the desired goals in terms of e-/e+ total stored currents, beam shapes and dimensions, transverse and longitudinal positions. Toroidal magnetic tools, electrostatic pickups, electromagnetic striplines or cavities, and synchrotron light monitors are the usual and in large part commercial devices used to know how many charges are in the ring, how they are distributed in the buckets, how much the bunches are unstable or misshaped for coupled bunch oscillations due to Coulomb's force and ring vacuum chamber impedance.
- The achievement of higher luminosity for the colliders or lower emittance for the synchrotron light source, needs to control at the best the beam characteristics and to identify any not foreseen behaviours. The diagnostics role is hence fundamental and always new tools need to be planned and put under investigations to follow the accelerator physicist requests. Furthermore it is important to note that while the beam diagnostics is based on turnkey and mature technologies, on the contrary the bunch-by-bunch diagnostics has state-of-art applications showing promising development perspective.

The abc: light from storage rings

- As well known, in a storage ring (like the e- DAFNE main ring) the beam, under the bending force of magnetic fields, looses energy (few keV in DAFNE) emitting the so called *synchrotron light*.
- Depending by the ring energy, the photons are spread in a large wavelength range but, due to the restoring radiofrequency (RF) field, they are always packed in photon bunches replicating the particle bunches.
- More precisely the RF signal has usually a sinusoidal shape with a frequency based on the ring lenght and the harmonic number.
- The RF sinusoidal field forces the charge to be distributed within a bucket as a gaussian or almost-gaussian bunch oscillating around an equilibrium point called synchronous phase.
- Diagnostic systems made by different technologies can be designed to evaluate the stored bunch pattern as well as the single bunch property.
- Goal of this lesson is to evaluate a simple infrared detector.

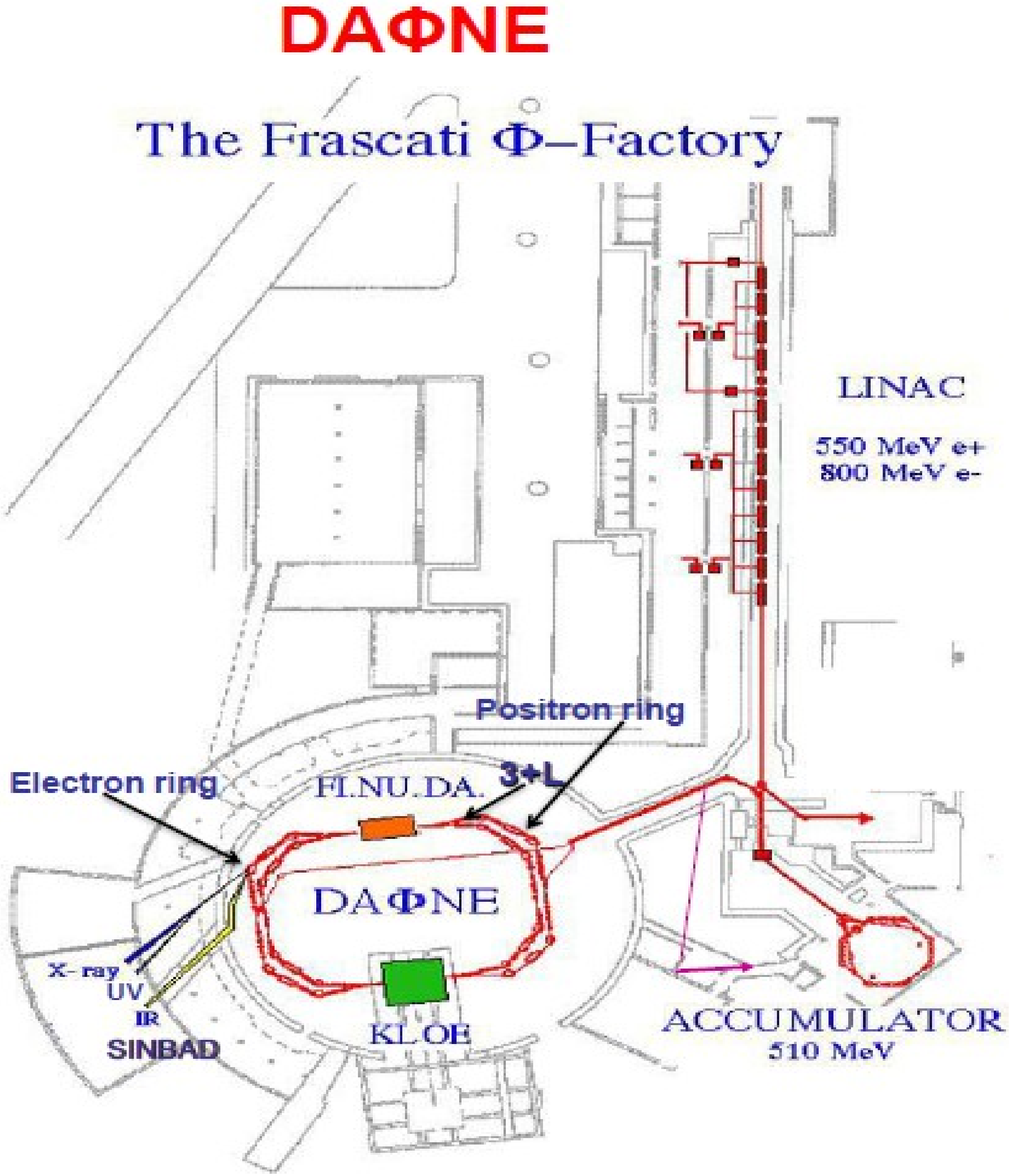

DAFNE has two infrared beamlines: SINBAD, from the electron stored beam (here we are);

3+L, from the positron stored beam, inside DAFNE hall: it cannot be visited during DAFNE operations.

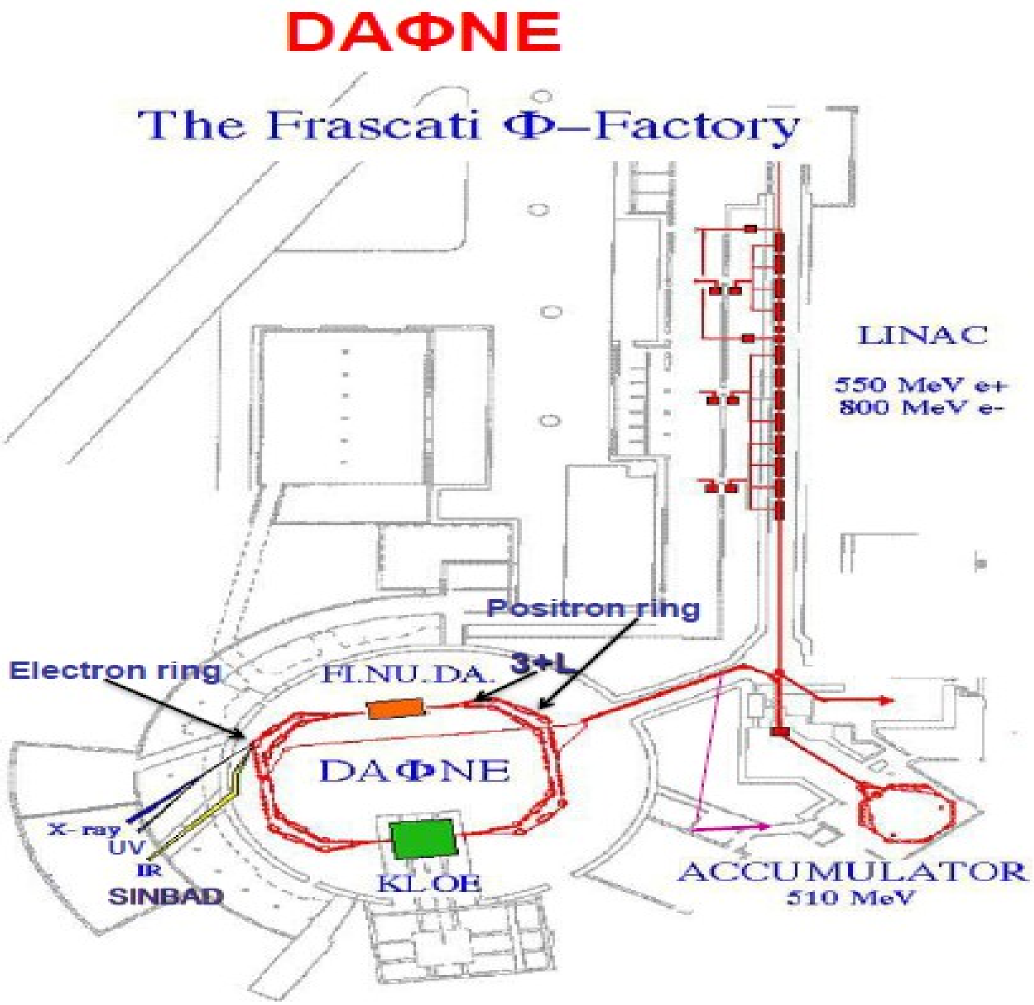

Some number on DAFNE:

Harmonic number H=120

RF frequency=368.667MHz

Revolution Frequency = RF/H=368.667/120=3.072MHz

Pattern usually injected: from bunch 1 to 103, with a gap of 17 empty buckets.

The gap is necessary to avoid the ion trapping.

The 3+L beamline with HV (High Vacuum) chamber before the installation of the optical table and the 5 mirrors

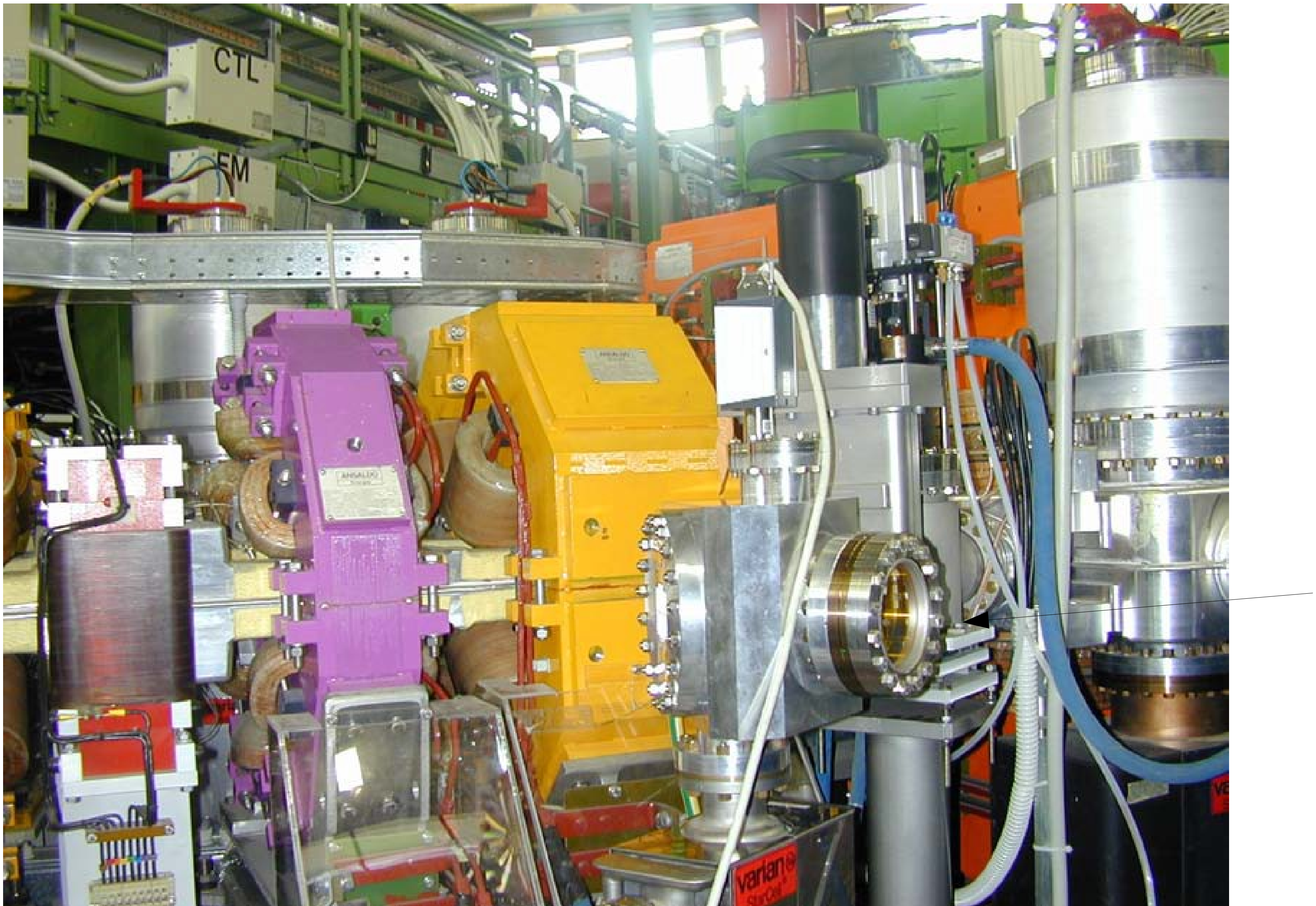

The source of SR light from e+ beam

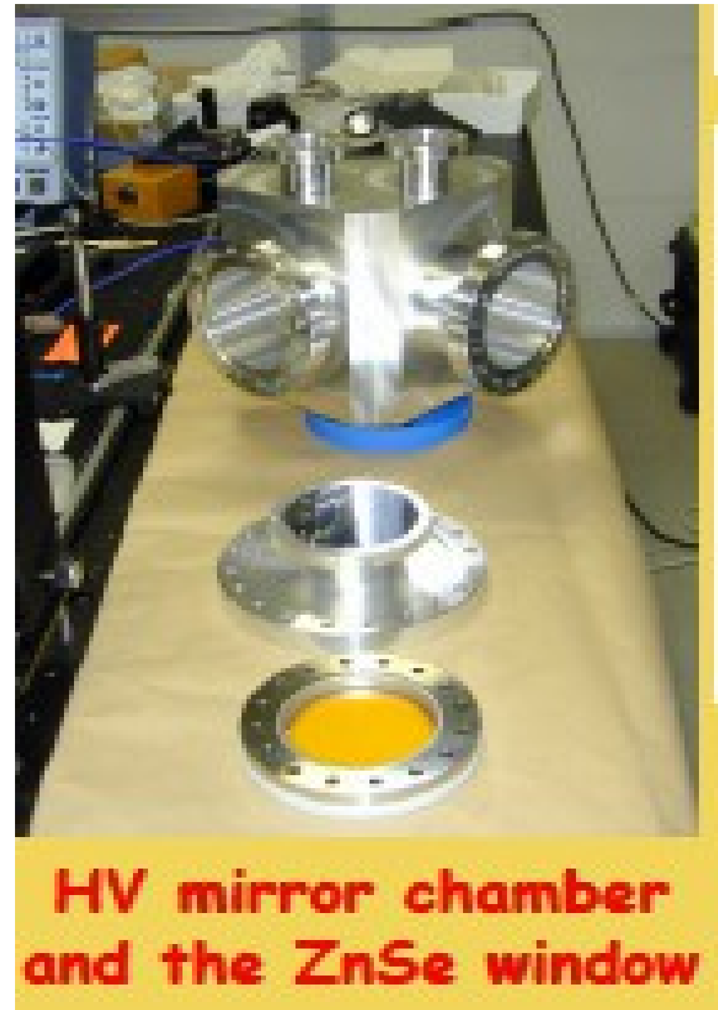

zinc- selenium window for infrared photons

The 3+L layout is designed considering the small available space

silica mirror in place of gold

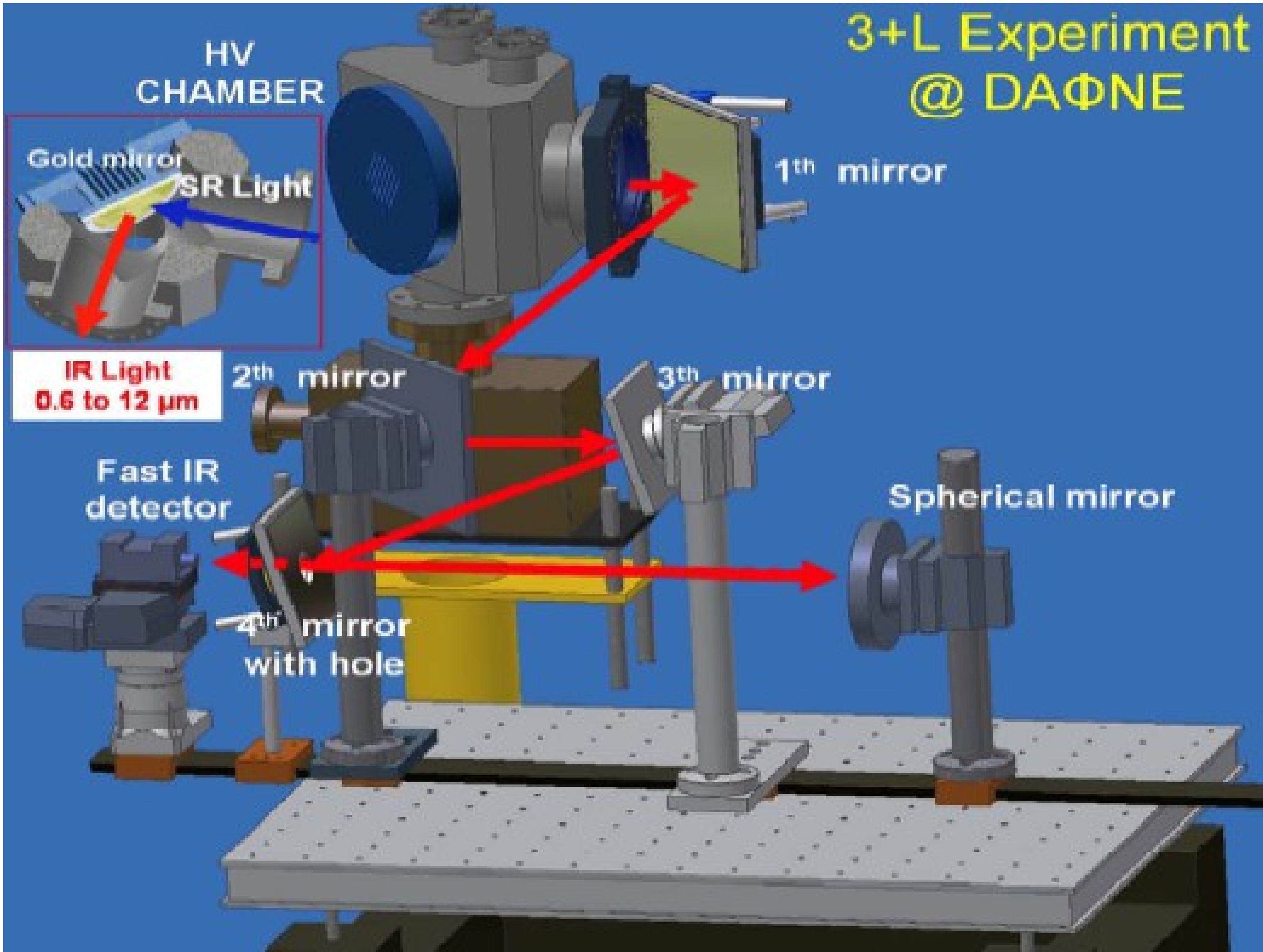

3+L beamline completely installed

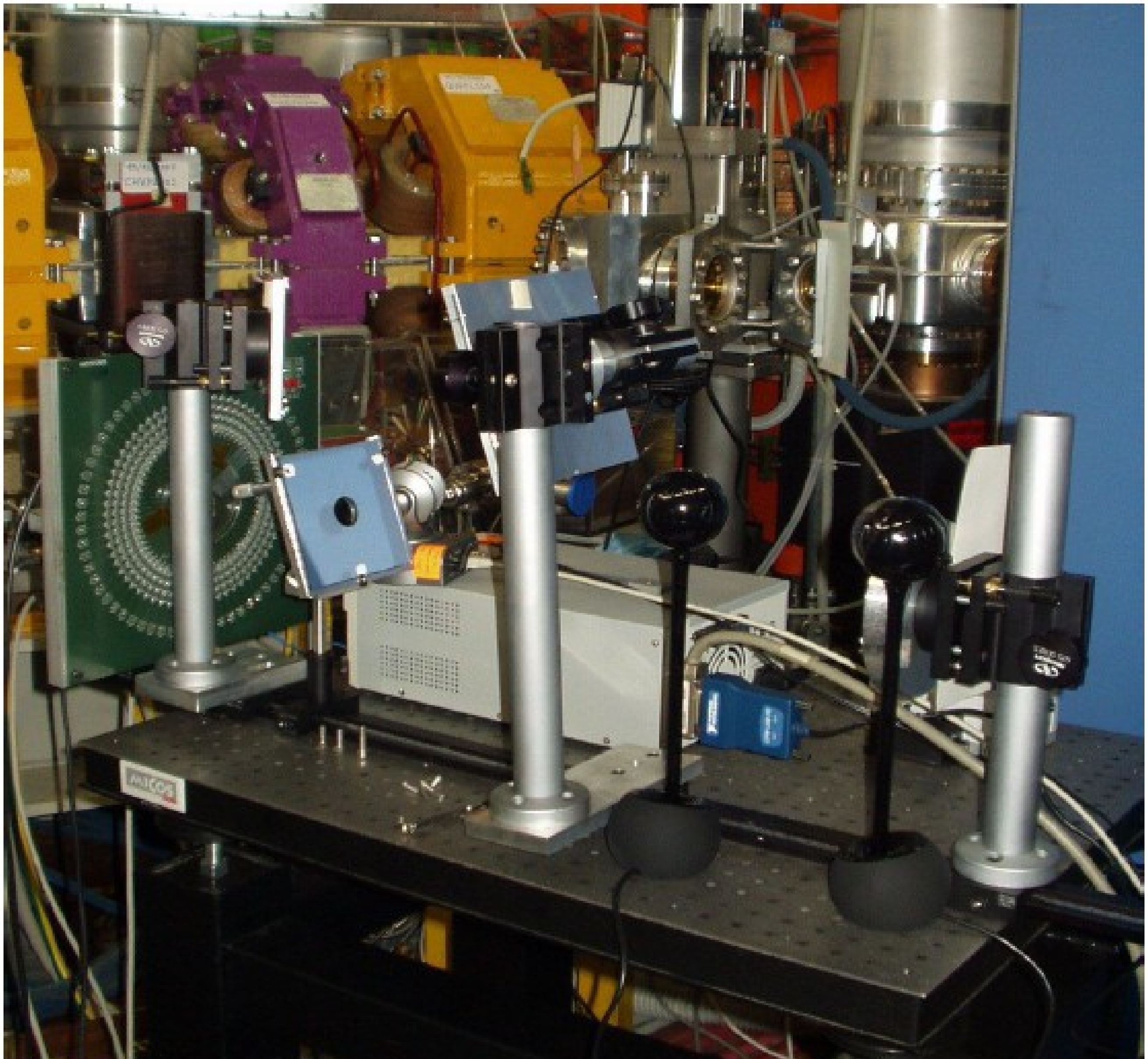

- On the left a special 2D detector with 2x32 pixels is placed (it is green and circular)

BEAM DIAGNOSTICS WITH SR

DIMENSIONS OF CROSS SECTION OF THE BEAM BY THE IMAGE OF SR EMISSION

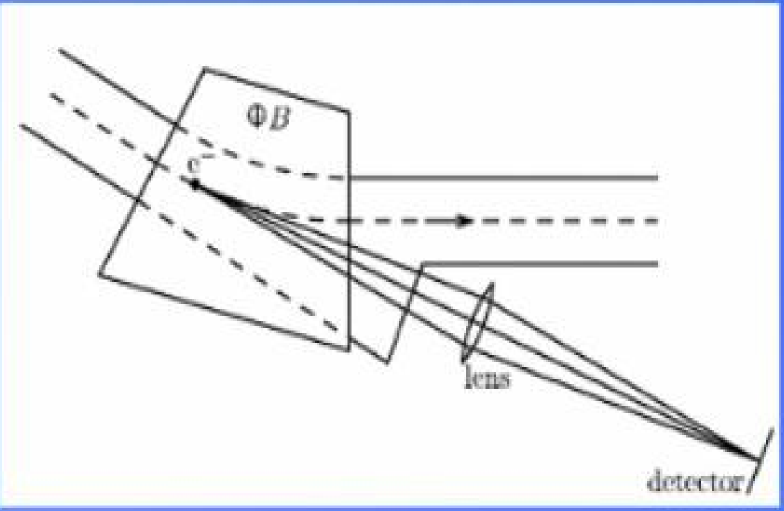

MEASURE OF THE ANGULAR SPREAD OF THE PARTICLES IN THE BEAM BY OBSERVATION OF THE DIRECT EMISSION

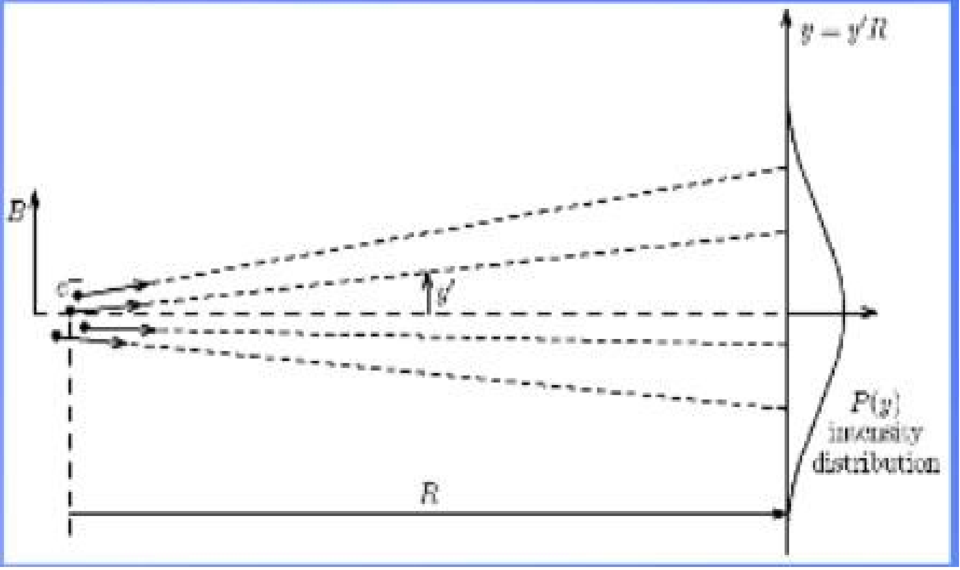

STATUS OF THE ART OF SR BEAM DIAGNOSTICS

MEASURE OF SR INTENSITY

FROM IMAGING OF SR EMISSION
BEAM PROFILE, BEAM POSITION
BEAM STABILITY AND DYNAMICS
CAN BE OBTAINED

SR MONITORS VUV, X-RAY
AND VISIBLE WAVELENTHGS

DETECTORS:
CCD /Si ARRAY/ PHOTODIODES

XBPMs

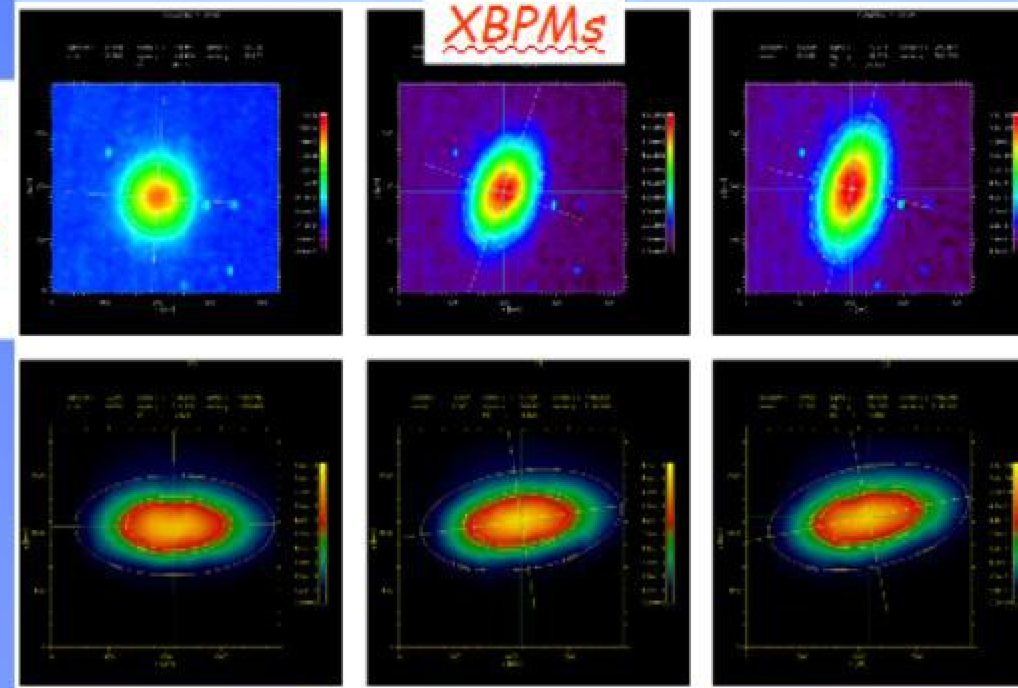

K.Holldack, BESSY

MEASURE OF TIME RESOLVED SR INTENSITY

FAST PHOTON DETECTORS
BUNCH LENGTH
MEASURAMENTS:
Sub-ns to ps response time

→ VERY FAST IR
UNCOOLED OR
PELTIER COOLED
PHOTODETECTORS

IR RADIATION AND PHOTON IR DETECTORS

Spectral Region	Wavelength Range (μm)
Near-Infrared	0.7 - 5
Mid-Infrared	5 - ~30

IR wavelengths definition for detectors

MWIR	3-5 micron
LWIR	8-14 micron

Quantum detectors fabricated with narrow-gap Semiconductors (intrinsic or extrinsic)

	Semiconductor Materials (intrinsic)	λ_t [μm]
Ternary narrow gap semiconductors	$Hg_xCd_{1-x}Te$	2 to 30
Binary narrow gap semiconductors	InSb	0.4 to 5.3

PHOTO DETECTORS RESPONSE TIME

Response time τ

Time for the detector output to fall to 1/e of the initial value when radiation is switched off

How fast a photo detector can respond to a pulse of optical radiation depends to:

Carrier lifetimes in semiconductors (majority or minority carriers)

Recombination time of carriers inside the semiconductor

Diffusion, drift and trapping of carriers inside the semiconductor

Transit time of photo generated carriers

RC constant of equivalent circuit

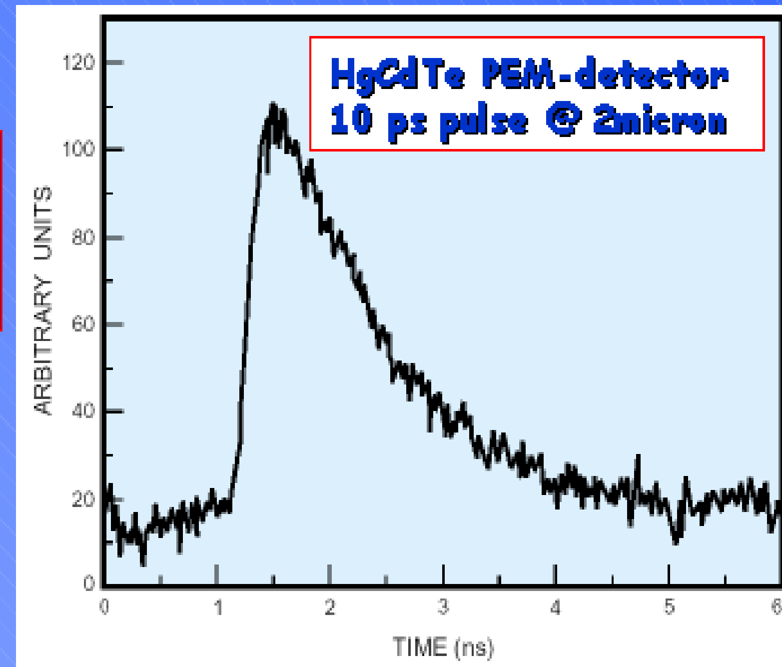

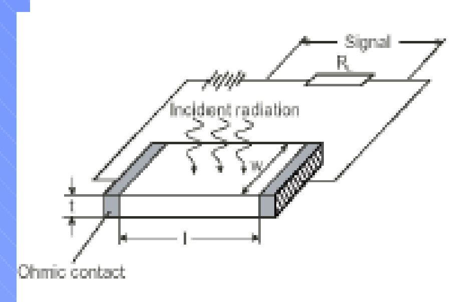

$D^* = (A_0 \Delta f)^{1/2}/NEP$

D* can be interpreted as S/N ratio out of a detector normalized to the detector area and bandwidth

In Photo-conductive detectors

$D^* \approx \tau^{1/2}$

IR DETECTORS SEMICONDUCTORS

HgCdTe
is the most
important semiconductor alloy
for Near-Mid-IR photon detection

Why?

High α/G (D*~ α/G)
High QE
Large tunable gap
λ cut-off 1-25 micron
(also dual band or multicolor detector)
Working also
at higher temperature

D* for thermal noise limited HgCdTe photodetectors

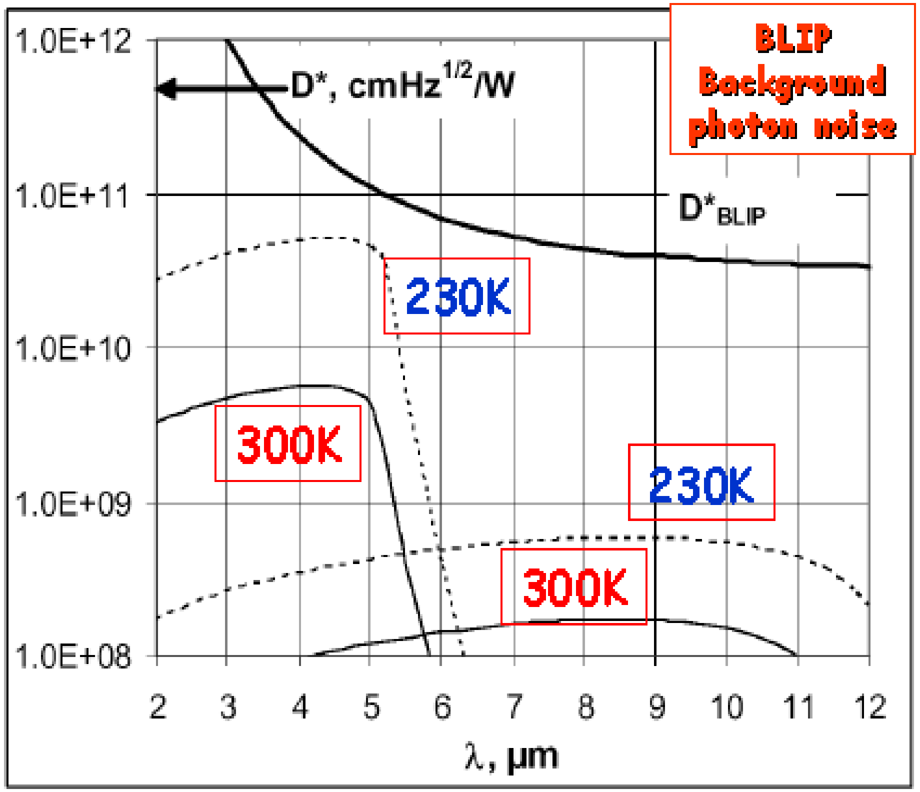

BLIP
Background photon noise

77 K BLIP PERFORMANCE
beetwen 2-20 micron

230 K (Peltier coolers)
Sub-BLIP for MWIR and LWIR

300 K
MWIR Sub-BLIP
LWIR
Two or more order of magnitude below BLIP performance

J.Piotrowski, 2nd Cephona Workshop, Warsaw, 2004

IR PHOTODETECTORS

MAIN PRINCIPLES OF GENERATION OF OPTICALLY CARRIERS IN PHOTODETECTORS

PHOTOCONDUCTIVE
PC
detectors

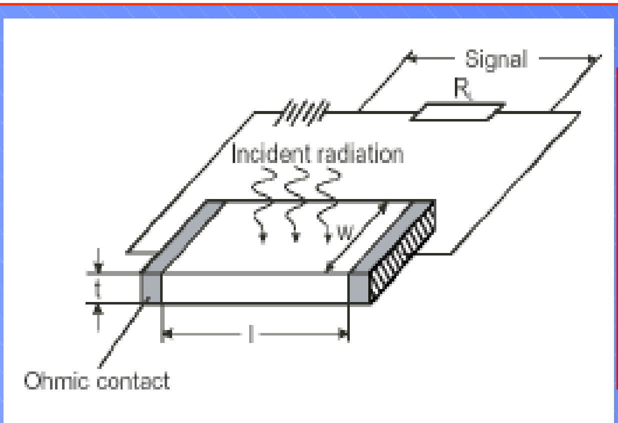

ELECTRICALLY BIASED DEVICES
SIGNAL GENERATED IN THE ABSORBER
BY CHANGE OF ITS RESISTENCE
OR
CONDUCTANCE

PHOTOELECROMAGNETIC
PEM
detectors

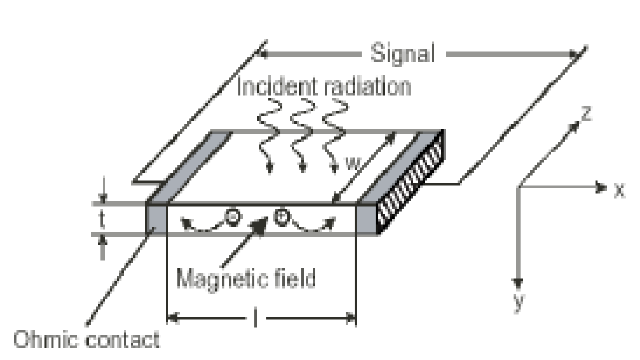

SIGNAL GENERATED
BY DIFFUSION OF
PHOTOGENERATED CARRIERS
DEFLECTED
BY A MAGNETIC FIELD
(2T, PERMANENT MAGNETS)

PHOTOVOLTAIC
PV
detectors

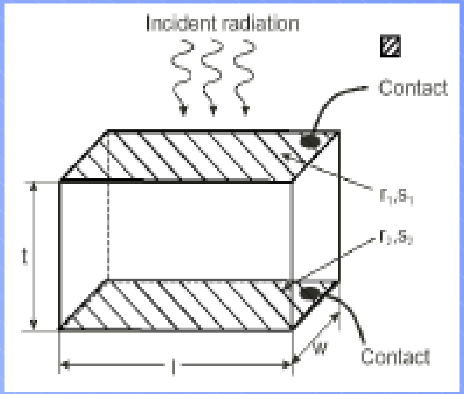

PHOTOVOLTAIC EFFECT
IN BIAS OR UNBIASED
HOMO OR HETEROJUNCTION

What we use

Photoconductors (PC)

Photoconductive Detectors based on the **Photoconductive Effect**. Infrared radiation generates charge carriers in the semiconductor active region decreasing its resistance. The resistance change is sensed as a voltage change by applying a constant current bias. The optimum bias current is specified in the **Final Test Report** and depends on the detector size, operating temperature and spectral characteristics.


INFRARED DETECTOR
Type
PC-10.6
No
14359
VIGO System S.A.
www.vigo.com.pl

Hg-Cd-Te detector (Mercury-Cadmium-Tellurium) on a GaAs layer

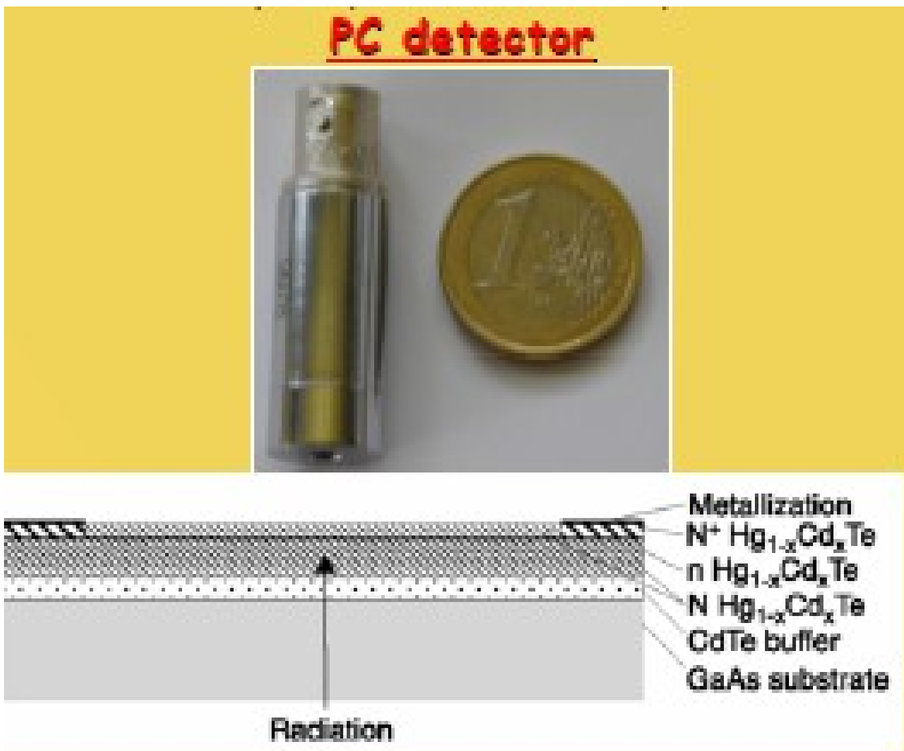

- The PC-λopt (λopt - optimal wavelength in micrometers) feature IR photoconductive detector.
- This series is easy to use, no cooling or heatsink needed. The devices are optimized for the maximum performance at λopt. Cut-on wavelength is limited by GaAs transmittance (~0.9 μm). Bias is needed to operate photocurrent. Performance at low frequencies (<20 kHz) is reduced due to 1/f noise. Highest performance and stability are achieved by application of variable gap (HgCd)Te semiconductor, optimized doping and sophisticated surface processing.
- Standard detectors are available in TO39 or BNC packages without windows. Various windows, other packages and connectors are available upon request.

PC Series 2 – 11 µm IR PHOTOCONDUCTORS

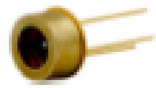

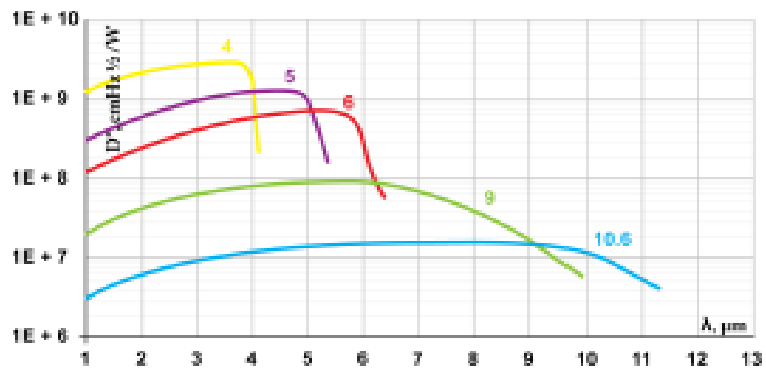

Example of D* vs Wavelength λ for PC Series HgCdTe Detectors. Spectral Characteristics of individual detectors may vary from those shown on the chart.

Features

- Ambient temperature operation
- Perfect match to fast electronics
- Convenient to use
- Wide dynamic range
- Low cost
- Prompt delivery
- Custom design upon request

Description

The PC-λ_{opt} (λ_{opt} - optimal wavelength in micrometers) feature IR photoconductive detector.

This series is easy to use, no cooling or heatsink needed. The devices are optimized for the maximum performance at λ_{opt}. Cut-on wavelength is limited by GaAs transmittance (~0.9 µm). Bias is needed to operate photocurrent. Performance at low frequencies (<20 kHz) is reduced due to 1/f noise. Highest performance and stability are achieved by application of variable gap (HgCd)Te semiconductor, optimized doping and sophisticated surface processing.

Standard detectors are available in TO39 or BNC packages without windows. Various windows, other packages and connectors are available upon request.

IR Detector Specification @20°C

Parameter	Symbol	Unit	PC-4	PC-5	PC-6	PC-9	PC-10.6
Optimal Wavelength	λ_{opt}	µm	4	5	6	9	10.6
Detectivity[1]: @ λ_{peak}, 20 kHz @ λ_{opt}, 20 kHz	D*	$\frac{cm\sqrt{Hz}}{W}$	≥3.2×10^9 ≥2.0×10^9	≥1.5×10^9 ≥1.0×10^9	≥7.0×10^8 ≥3.0×10^8	≥1.0×10^8 ≥2.0×10^7	≥1.5×10^7 ≥9.0×10^6
Voltage Responsivity - Width Product @λ_{opt}, 1×1mm	$R_v \cdot w$	$\frac{V\,mm}{W}$	≥100	≥40	≥6	≥0.4	≥0.1
Time Constant	τ	ns	≤1000	≤500	≤200	≤2	≤1
Corner Frequency	1/f	kHz	1 to 20				
Bias Current - Width Ratio	$\frac{I_b}{w}$	$\frac{mA}{mm}$	1 to 5	1 to 10	1 to 15	2 to 20	5 to 30
Sheet Resistance	$R_\square$	Ω/□	300 to 1000	200 to 400	100 to 300	50 to 150	40 to 120
Operating Temperature	T	K	~300				
Acceptance Angle, F/#	Φ, -	deg, -	~90, 0.71				

[1] Data Sheet states minimum guaranteed D* values for each detector model. Higher performance detectors can be provided upon request.

Type	Optical Area (mm×mm)									
	0.025×0.025	0.05×0.05	0.1×0.1	0.2×0.2	0.25×0.25	0.5×0.5	1×1	2×2	3×3	4×4
PC-4	X	X	X	X	X	X	X	X	X	X
PC-5	X	X	X	X	X	X	X	X	X	X
PC-6	X	X	X	X	X	X	X	X	X	X
PC-9	X	X	X	X	X	X	X	X	X	X
PC-10.6	X	X	X	X	X	X	X	X	X	X

X – standard detectors

Schematics

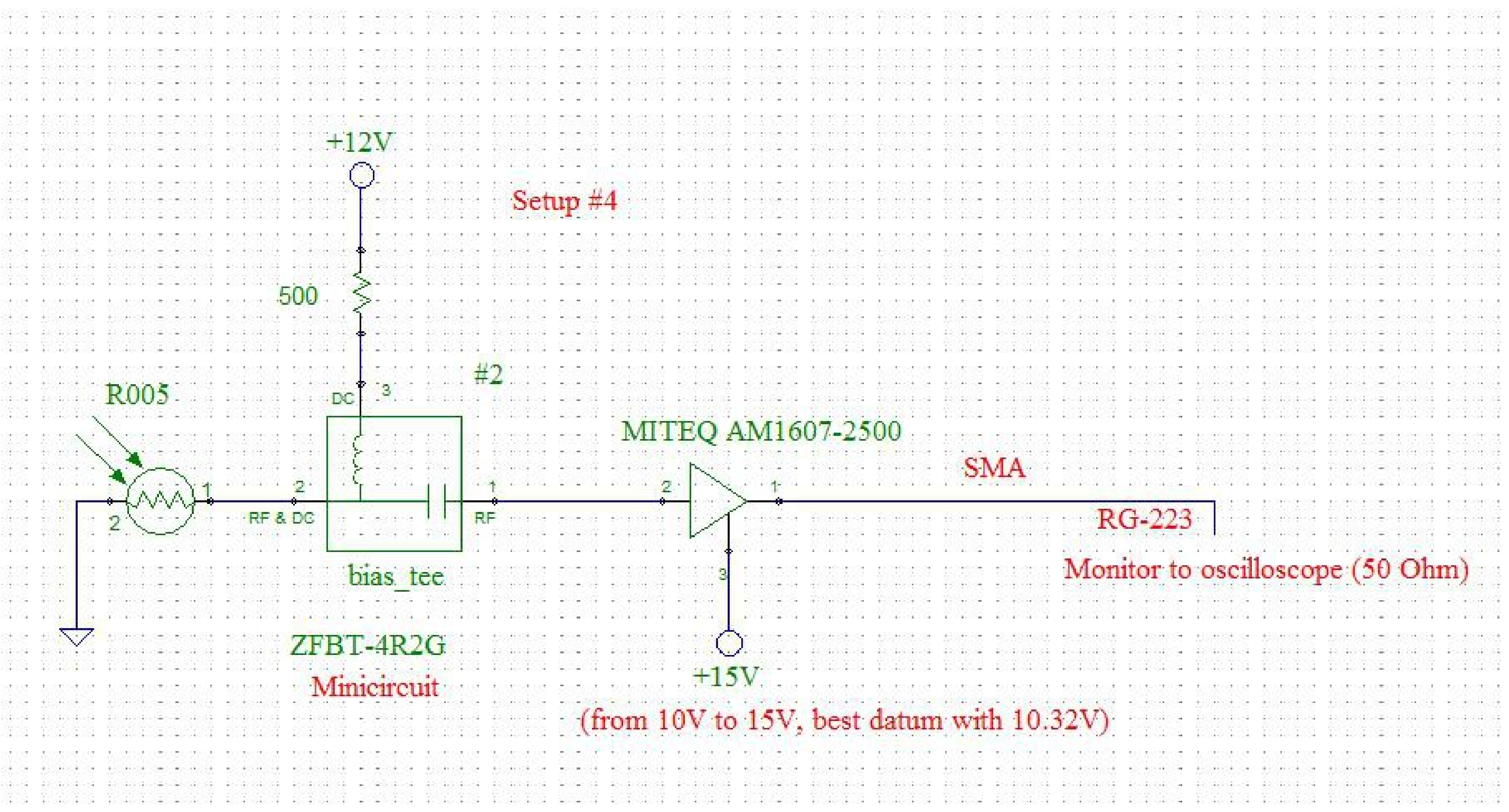

+12V
Setup #4
500
#2
R005
DC
3
MITEQ AM1607-2500
SMA
1
2
RF & DC
1
RF
2
1
RG-223
3
bias_tee
Monitor to oscilloscope (50 Ohm)
ZFBT-4R2G
Minicircuit
+15V
(from 10V to 15V, best datum with 10.32V)

Bias-Tee

Coaxial

Bias-Tee

ZFBT-4R2G+

50Ω Wideband 10 to 4200 MHz

CASE STYLE: K18

Connectors	Model	Price	Qty.
SMA	ZFBT-4R2G+	$89.95	(1-9)
BRACKET (OPTION "B")		$5.00	(1+)

+RoHS Compliant

Maximum Ratings

Operating Temperature	-55°C to 100°C
Storage Temperature	-55°C to 100°C
RF Power	30 dBm max.
Voltage at DC port	30 V max.
Input Current	500 mA
DC resistance from DC to RF&DC port	4.5 ohm typ.

Permanent damage may occur if any of these limits are exceeded.

Coaxial Connections

RF	1 (SMA female)
RF&DC	2 (SMA male)
DC	3 (SMA female)

Features
- wideband, 10 to 4200 MHz
- low insertion loss, 0.6 dB typ.
- good isolation, 40 dB typ.

Applications
- biasing amplifiers
- biasing of laser diodes
- biasing of active antennas
- DC return
- DC blocking
- test accessory

Bias-Tee Electrical Specifications

FREQUENCY (MHz)		INSERTION LOSS* (dB)						ISOLATION* (dB) (RF port to DC port) (RF&DC port to DC port)						VSWR** (:1)					
		L		M		U		L		M		U		L		M		U	
f_L	f_U	Typ.	Max.	Typ.	Max.	Typ.	Max.	Typ.	Min.	Typ.	Min.	Typ.	Min.	Typ.	Max.	Typ.	Max.	Typ.	Max.
10	4200	0.15	0.6	0.6	1.2	0.6	1.6	32	20	40	20	30	20	1.05	1.2	1.13	1.3	1.13	1.3

L = low range (f_L to 10 f_L) M = mid range (10 f_L to f_U/2) U = upper range (f_U/2 to f_U)

* Insertion Loss and Isolation are guaranteed up to 30 dBm RF power and 200mA DC current.

** VSWR measured with open and short at DC port.

Typical Performance Data

Freq. (MHz)	Pin (dBm)	INSERTION LOSS (dB) with Current						ISOLATION (dB) (Pin= -10dBm) with current						VSWR (:1)
		0mA	20mA	50mA	100mA	150mA	200mA	10mA	20mA	50mA	100mA	150mA	200mA	
0.10	12.30	0.17	0.17	0.16	0.17	0.20	0.21	19.16	19.04	17.33	14.53	12.66	11.25	1.16
0.27	12.30	0.13	0.13	0.13	0.14	0.14	0.15	25.36	25.53	24.52	21.43	19.21	13.16	1.07
0.55	12.30	0.12	0.12	0.12	0.11	0.11	0.11	28.17	28.36	28.36	26.13	24.40	23.37	1.04
1.05	12.30	0.13	0.13	0.12	0.11	0.12	0.12	30.31	30.21	30.26	29.62	28.62	27.92	1.02
10.00	13.50	0.16	0.17	0.17	0.16	0.16	0.16	30.06	30.07	30.07	30.20	30.33	30.36	1.04
111.75	12.50	0.22	0.25	0.21	0.22	0.22	0.22	34.15	34.19	34.27	33.99	33.33	33.59	1.07
381.25	12.70	0.30	0.35	0.33	0.32	0.33	0.33	44.65	44.61	44.25	43.90	43.91	43.74	1.06
745.25	13.70	0.28	0.31	0.30	0.29	0.29	0.29	51.19	50.50	50.16	50.65	51.69	52.17	1.06
952.75	13.20	0.31	0.33	0.33	0.31	0.32	0.33	40.75	40.30	40.27	40.27	40.25	40.25	1.11
1531.25	13.00	0.46	0.43	0.47	0.46	0.43	0.49	42.53	42.59	43.34	43.77	44.36	44.17	1.13
2000.25	17.10	0.46	0.43	0.47	0.46	0.46	0.47	45.16	45.37	45.73	45.43	46.14	45.23	1.12
2551.00	14.40	0.40	0.42	0.41	0.42	0.43	0.41	53.15	53.72	52.19	53.17	52.67	53.67	1.12
3097.75	14.20	0.45	0.43	0.47	0.46	0.46	0.49	52.16	52.25	51.55	51.33	51.46	50.99	1.09
3565.25	15.10	0.73	0.74	0.75	0.75	0.75	0.75	46.72	47.19	46.36	45.53	46.19	45.65	1.07
4200.00	17.90	1.04	1.07	1.07	1.06	1.05	1.05	28.12	28.33	28.24	28.11	28.01	27.92	1.09
4502.50	-0.60	1.17	1.19	1.16	1.19	1.17	1.16	28.15	28.10	28.06	27.96	27.74	27.37	1.14
4792.00	-0.70	1.26	1.26	1.27	1.25	1.22	1.20	37.96	38.01	38.19	37.96	37.53	37.51	1.12
5221.75	-1.10	1.19	1.17	1.16	1.13	1.11	1.09	49.65	51.04	49.12	49.37	49.13	43.19	1.11
5550.75	-2.00	1.65	1.63	1.60	1.56	1.54	1.51	33.44	33.36	33.36	33.07	37.35	33.19	1.10
6000.00	-2.40	1.70	1.71	1.65	1.59	1.54	1.50	34.37	34.36	34.23	34.10	34.19	34.43	1.12

Outline Drawing

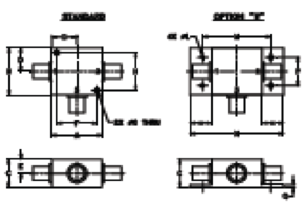

Outline Dimensions (inch / mm)

A	B	C	D	E	F	G	H
1.25	1.25	.75	.63	.38	1.00	.125	1.000
31.75	31.75	19.05	16.00	9.65	25.40	3.18	25.40

J	K	L	M	N	P	Q	wt
—	—	.125	1.688	2.18	.75	.07	grams
..	..	3.18	42.88	55.37	19.05	1.78	70.0

Electrical Schematic

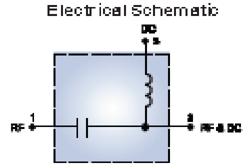

Performance Charts ZFBT-4R2G+

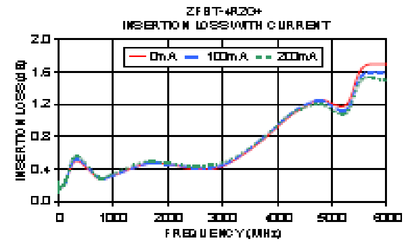

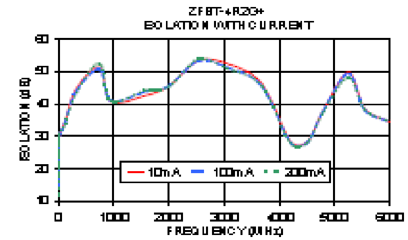

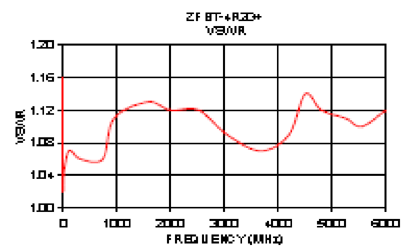

Mini-Circuits®
www.minicircuits.com P.O. Box 350166, Brooklyn, NY 11235-0003 (718) 934-4500 sales@minicircuits.com

Model: AM-1607-2500

Get A Quote

Description:	Amplifier
Specifications at	23 °C:
Frequency:	0.00001 to 2.5 GHz
Gain:	40 dB min.
Gain Flatness:	1.5 dB+/- max.
Noise Figure:	4.3 dB max.
Noise Temperature:	438.4 K max.
VSWR In:	2:1 max.
VSWR Out:	2:1 max.
P1dB Out:	8 dBm min.
Output IP3 Typ.:	18 dBm
Voltage:	15 V nom.
Current:	100 mA nom.
Outline Drawing:	179685-2
Operating Temp:	-30 to 75 °C

Get A Quote

Documents for AM-1607-2500
Outline Drawing: 179685 (PDF)

ITAR: NO

return to previous page

Similar Models

AM-1607-1000
AM-1607-2000
AM-1607-3000

Data from DAFNE e- beam

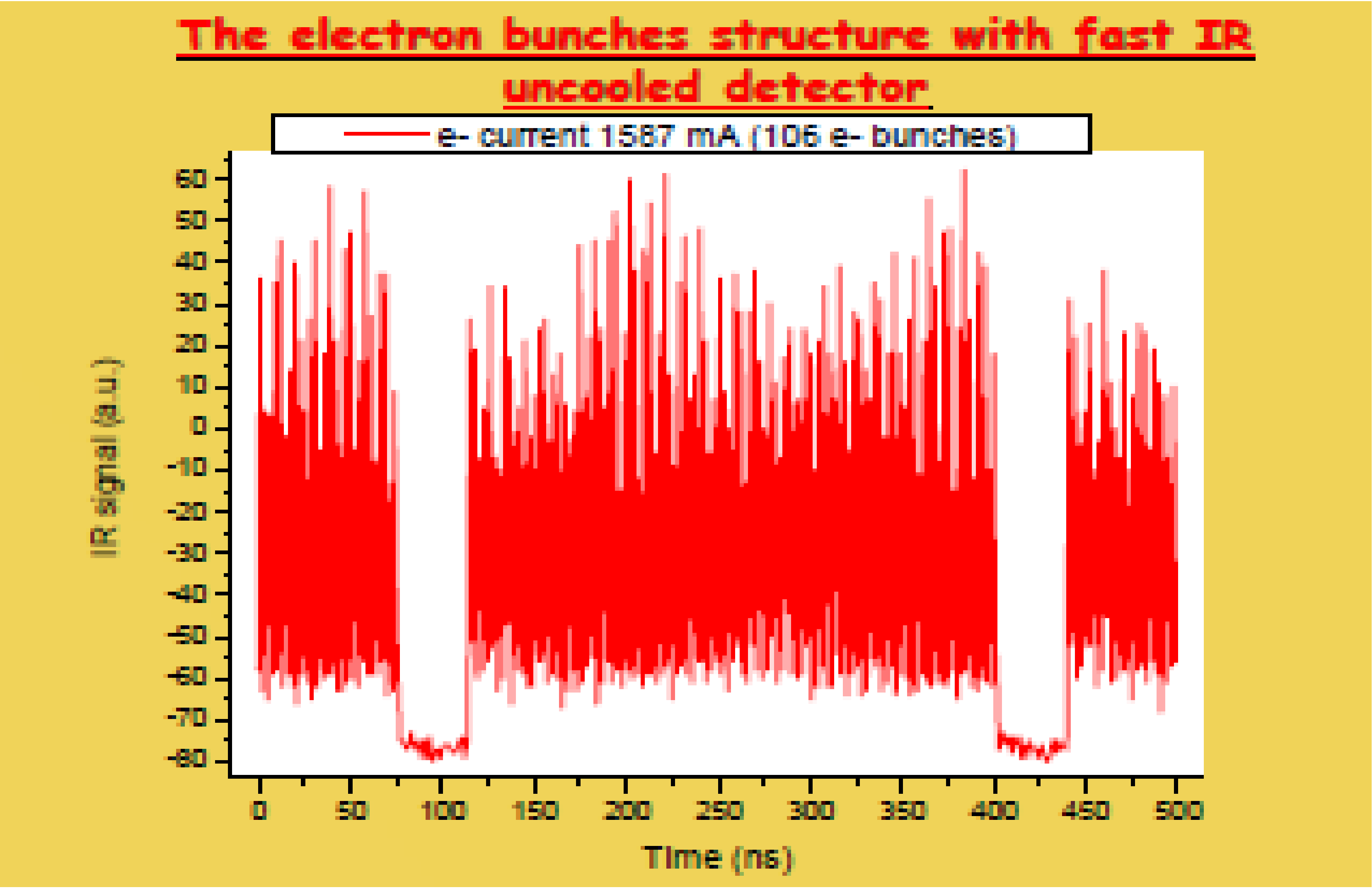

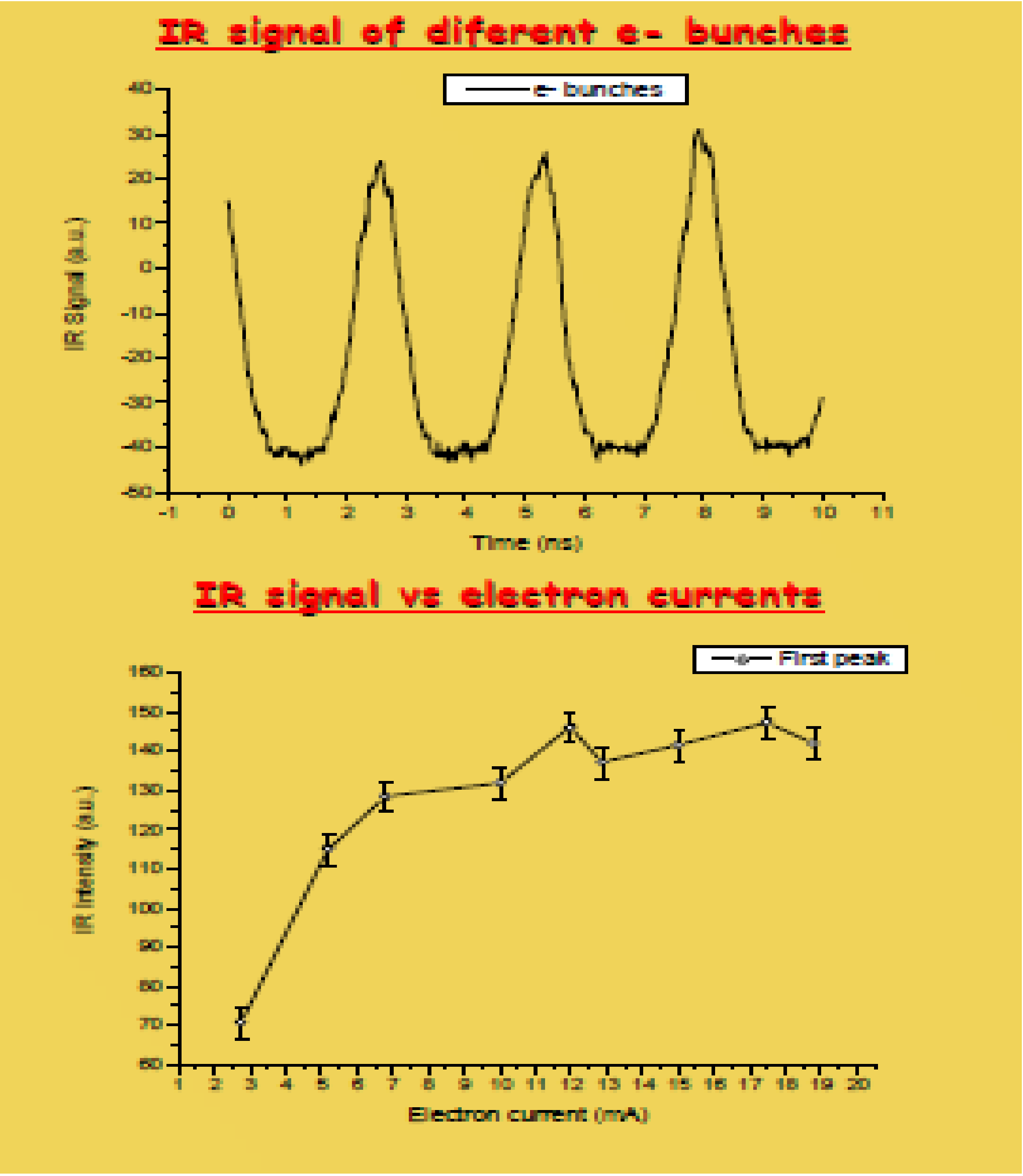

3 bunches in longitudinal by IR detection

Linearity of the detector

Frequency domain by IR detector

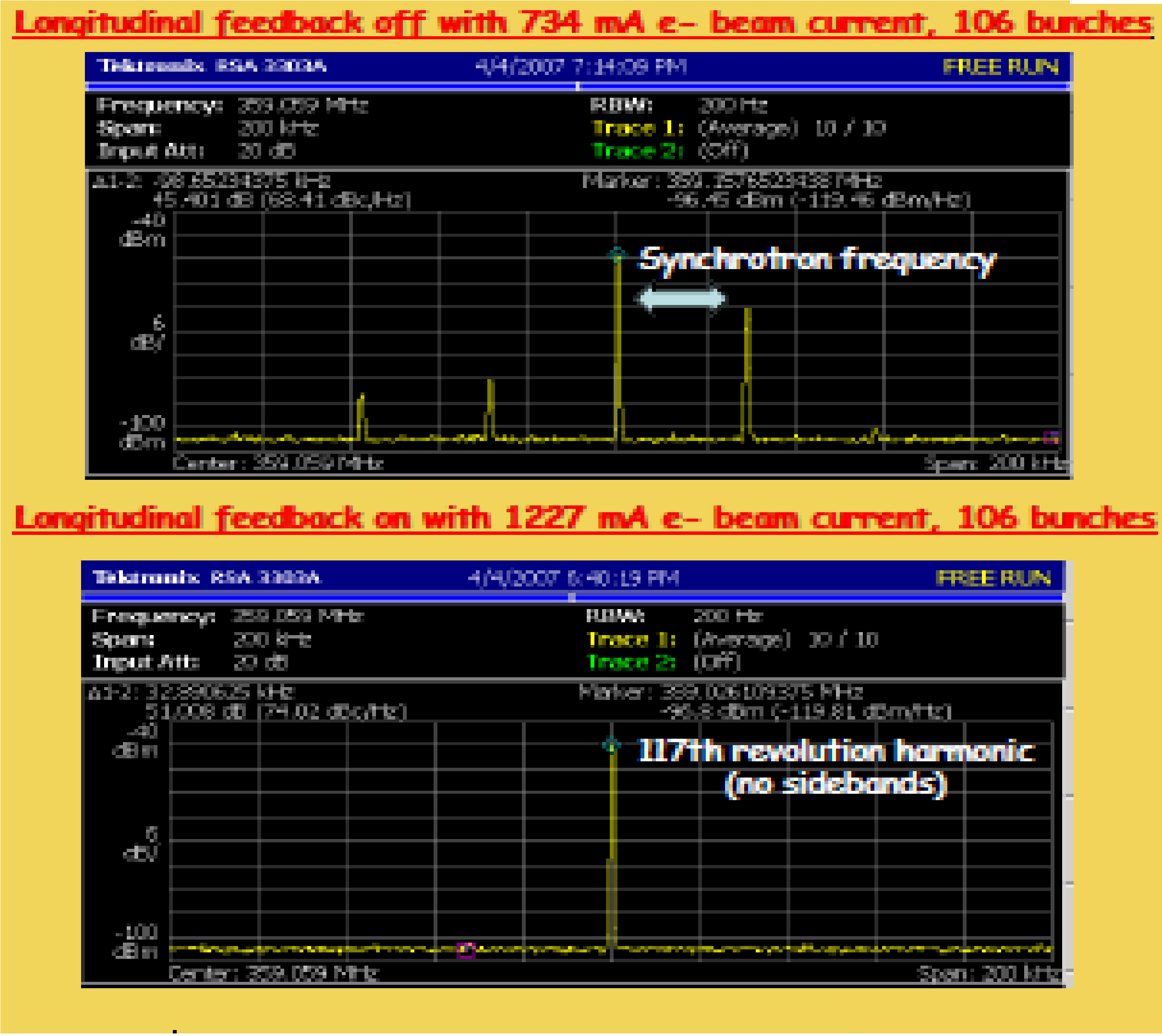

- Upper figure: longitudinal feedback off and the beam shows synschrotron sidebands
- Second plot: longitudinal feedback on, no synchrotron sidebands

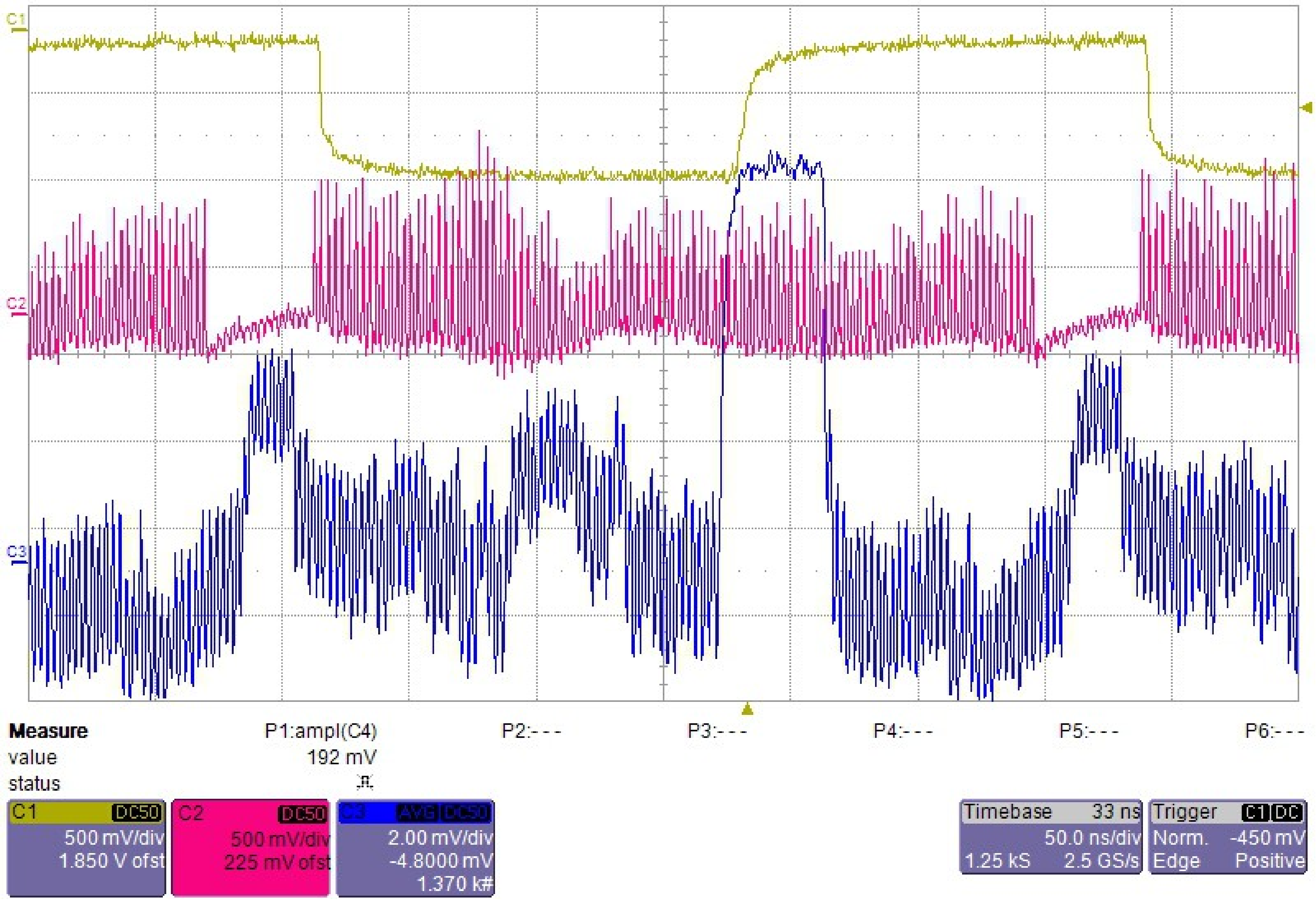
C1
C2
C3
Measure
P1:ampl(C4)
P2:- - -
P3:- - -
P4:- - -
P5:- - -
P6:- - -
value
192 mV
status
C1 DC50
500 mV/div
1.850 V ofst
C2 DC50
500 mV/div
225 mV ofst
C3 AVG DC50
2.00 mV/div
-4.8000 mV
1.370 k#
Timebase 33 ns
50.0 ns/div
1.25 kS 2.5 GS/s
Trigger C1 DC
Norm. -450 mV
Edge Positive

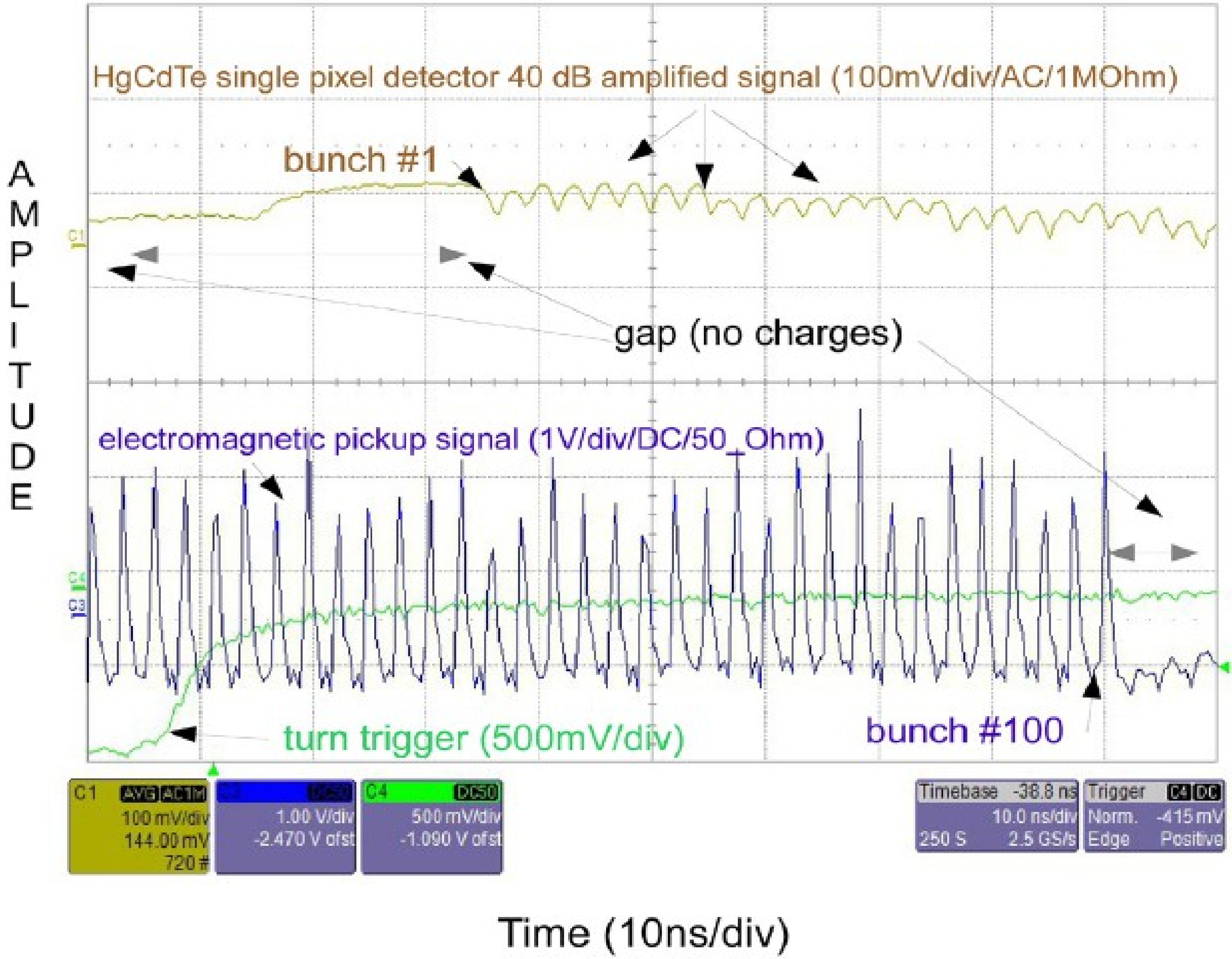

Figure 11. DAΦNE data taking at SINBAD on 13 June 2014. The traces are: the ring revolution or turn trigger (green), the beam signal from an electromagnetic pickup (blue, not amplified) and from one HgCdTe single pixel detector (yellow) amplified by 40 dB. The horizontal scale is 10 ns while the vertical scales are 0.5 V/div for the trigger (green), 1 V/div for e.m. pickup signal (blue) and 0.1 V/div for the IR detector signal (yellow). This last trace is coupled in ac and terminated to 1 MΩ while the other two are in dc at 50 Ω. This is to plot better the IR detector trace that has small amplitude. The blue signal shows the last bunches of the train before the gap while the yellow trace shows the first part of the bunch train. Note that beam data have been collected in different ring locations.

2x32 pixel detector

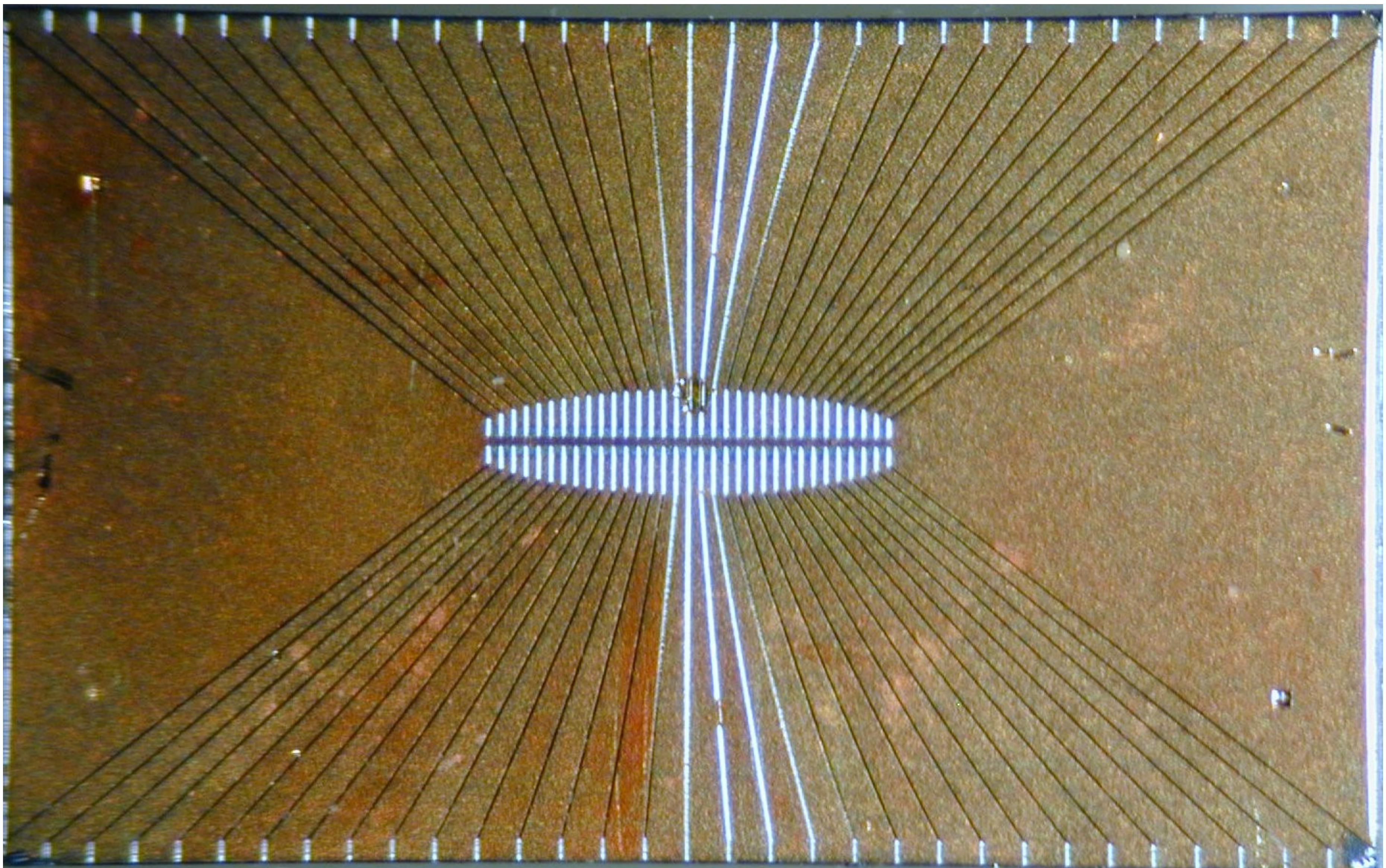

2x16 pixel detector

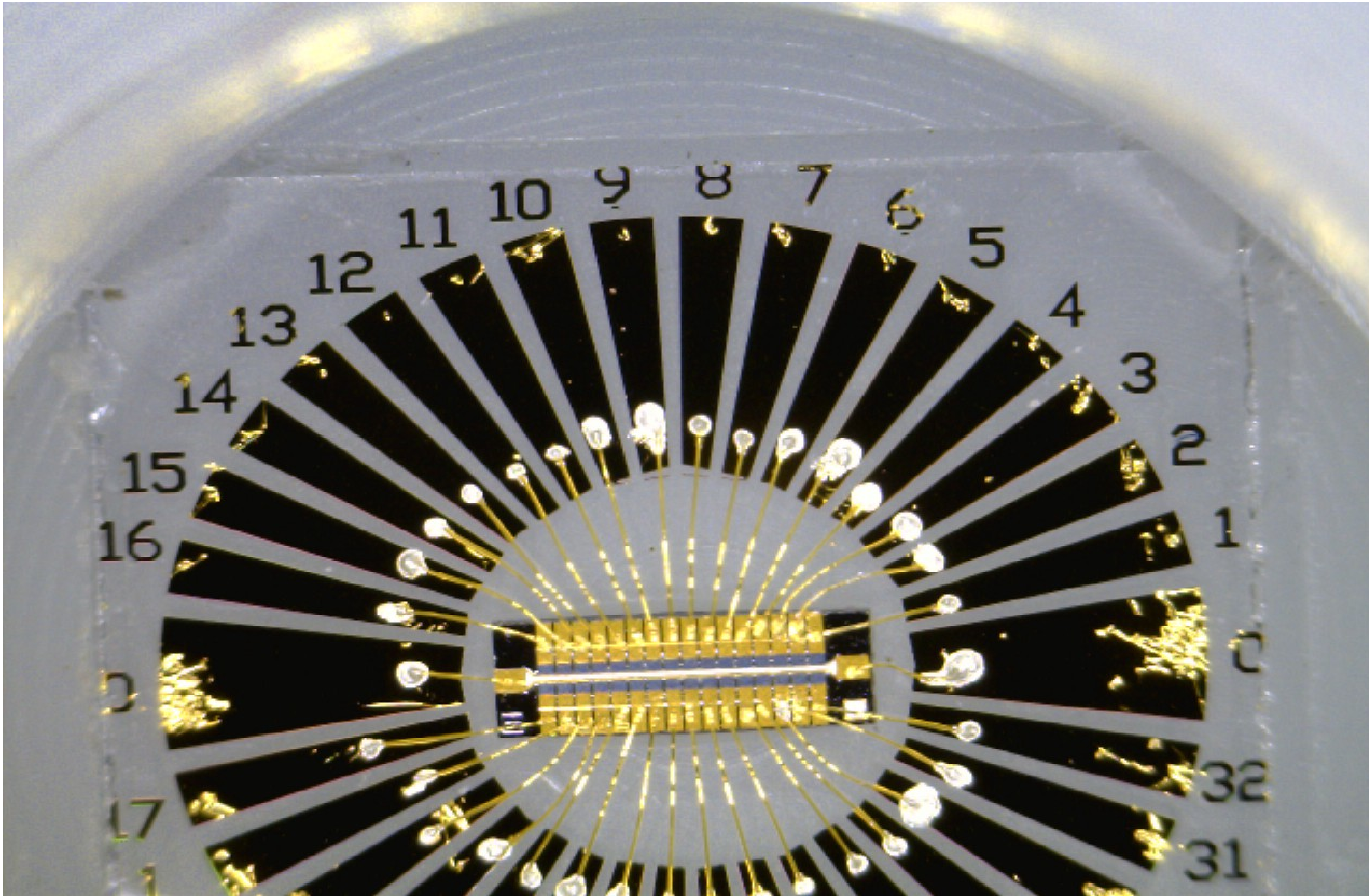

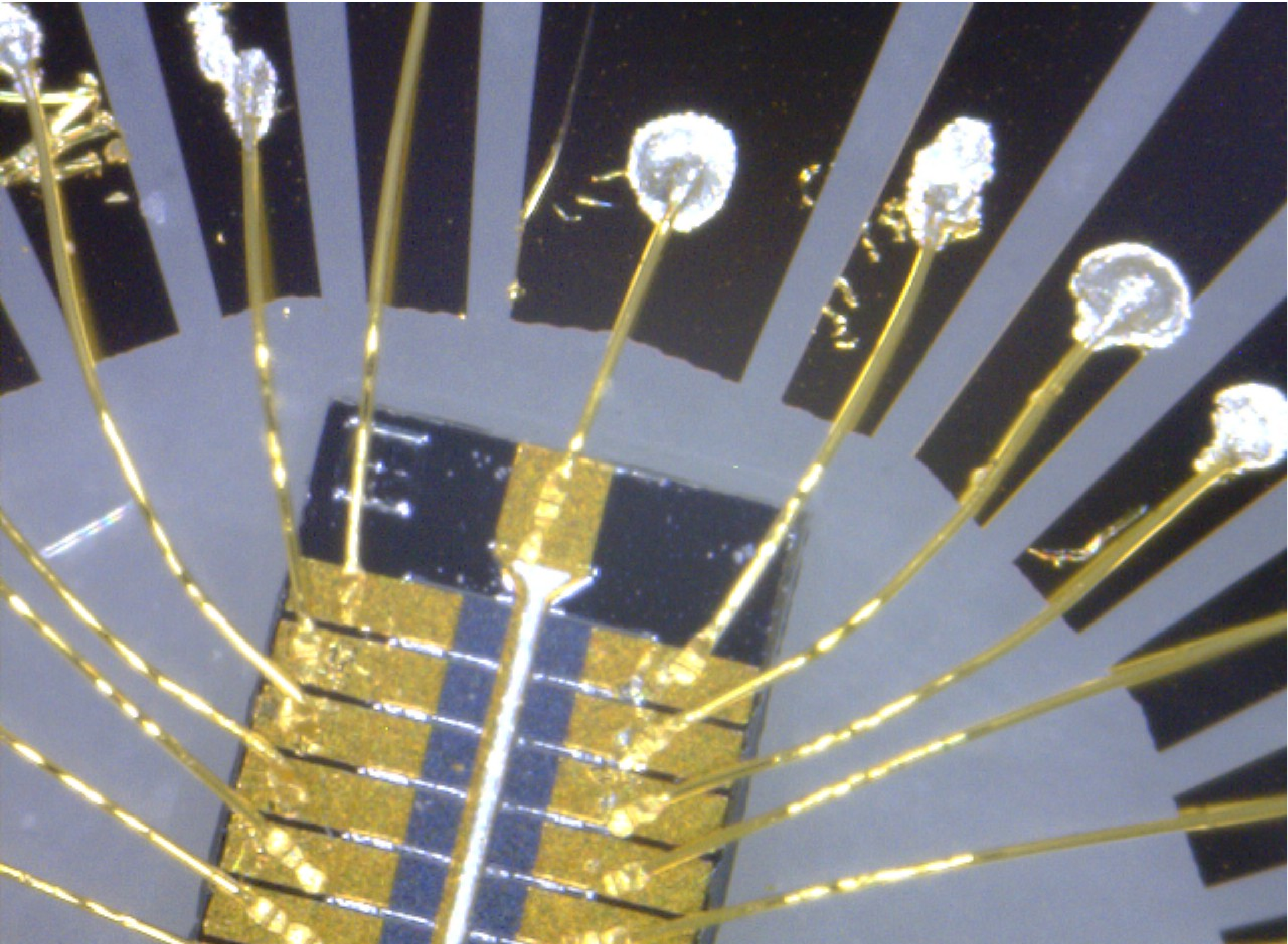

- This is the pcb (printed circuit board) where the 2x16 pixel is placed

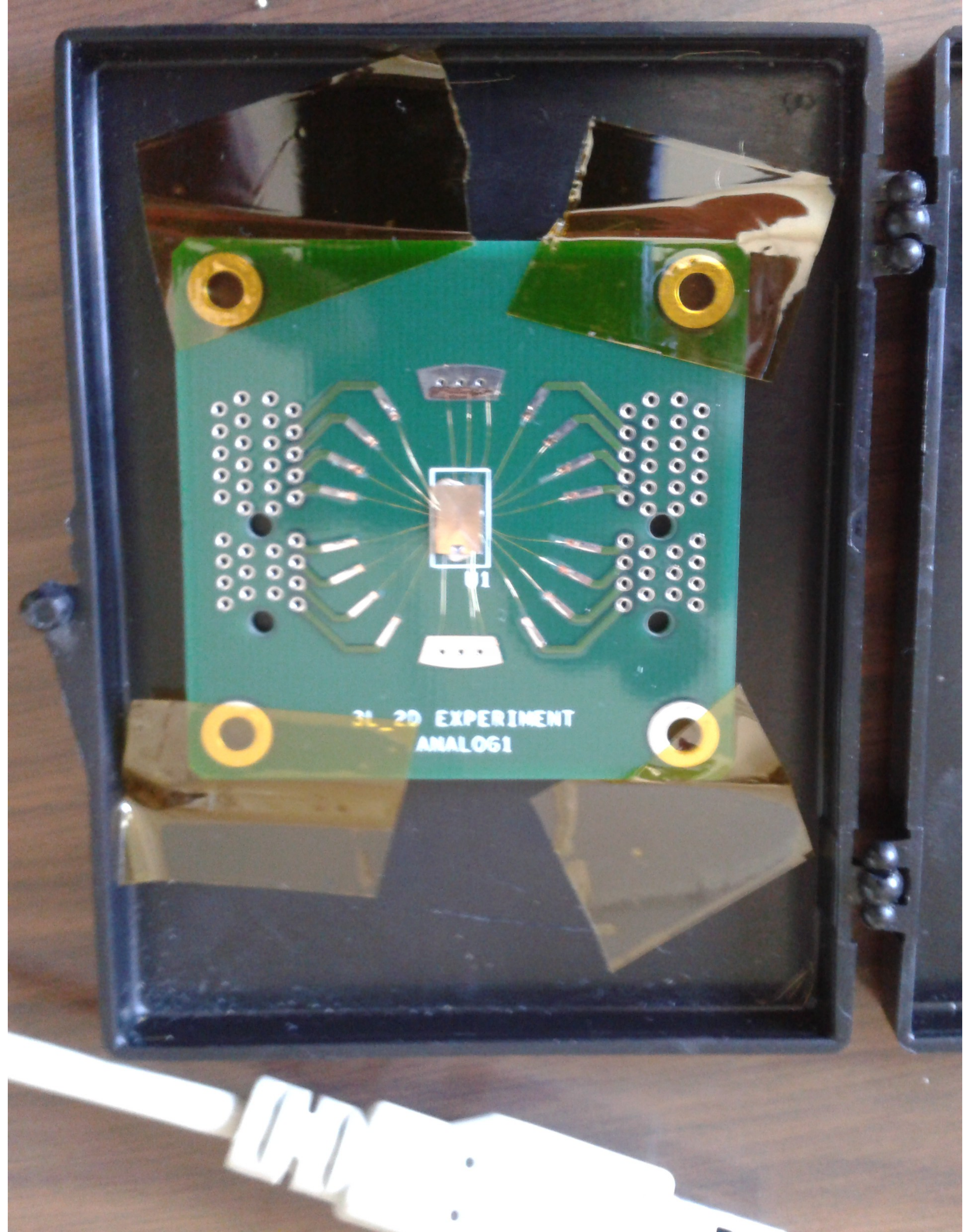

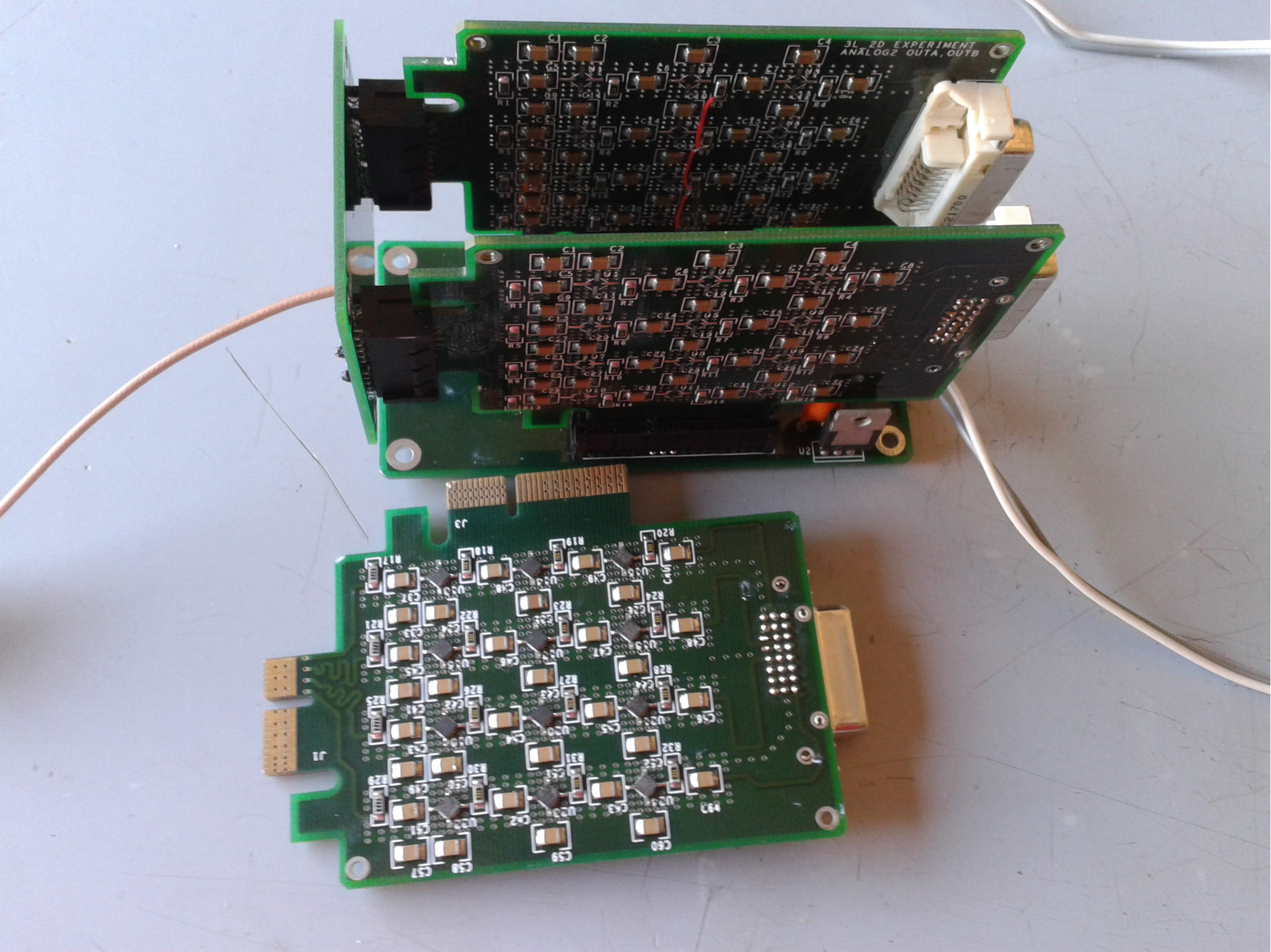
3L 2D EXPERIMENT
ANALOG2 OUTA,OUTB

- This is the timing module with 8 delay lines to deskew the sampling frequency (368 Mhz) for each pixel

FPGA acquisition system

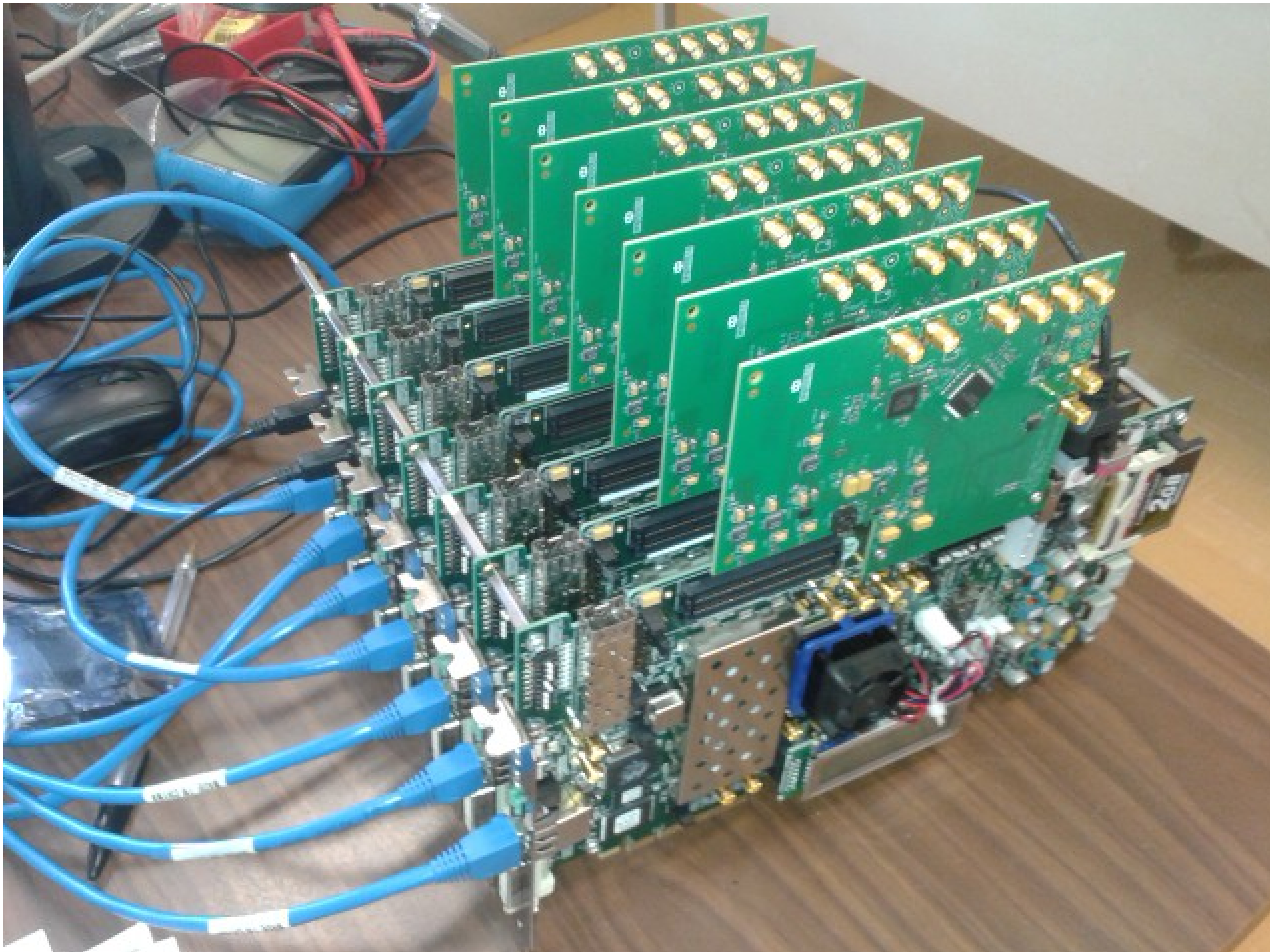

IOP Publishing Measurement Science and Technology
Meas. Sci. Technol. 26 (2015) 094003 (10pp) doi:10.1088/0957-0233/26/9/094003

Bunch-by-bunch profile diagnostics in storage rings by infrared array detection

A Drago[1], A Bocci[2], M Cestelli Guidi[1], A De Sio[3], E Pace[4] and A Marcelli[1]

[1] INFN-Laboratori Nazionali di Frascati, Via E. Fermi 40, Frascati (RM)
[2] Cesop Communication S.r.l, Via San Felice 13, 40122 Bologna, Italy
[3] INAF, Osservatorio Astrofisico di Arcetri, Largo E. Fermi 5, 50125 Firenze
[4] Universita' di Firenze, Largo E. Fermi 5, 50125 Firenze

E-mail: alessandro.drago@inf.infn.it

Received 17 November 2014, revised 11 May 2015
Accepted for publication 27 May 2015
Published 21 July 2015

Abstract
The latest generation of storage rings, both light sources and colliders, needs improved diagnostics systems to achieve the challenging design parameters. Although many commercially available diagnostics can be used to characterize performance in real time, modern high-luminosity and low-emittance accelerators need much more sophisticated and sensitive diagnostics devices. DAΦNE (Double Annular Φ-Factory for Nice Experiments), the LNF (Laboratori Nazionali di Frascati) e^+/e^- Φ-factory, is a collider working at an energy of 1.02 GeV in the centre of mass. The existing luminosity diagnostics at DAΦNE cannot explain the 30% discrepancy between the extrapolated 10-bunch peak luminosity and the standard fill pattern made by colliding 100 bunches. Ruling out the presence of nonlinear contributions and/or saturation of the existing KLOE (Kaon Long Experiment) detector when used as a precision luminosity monitor, new diagnostic approaches are needed. Here we describe the technique that we introduced at DAΦNE based on multi-pixel time-resolved infrared detectors. Preliminary results are presented and discussed.

Ready to get beam data ?